

## Measurement of plasma response to $n=2$ fields using saddle loops on JET

N. Wang<sup>1,2,\*</sup>, Y. Liang<sup>1</sup>, S. Gerasimov<sup>3</sup>, P. Denner<sup>1</sup>, P. Drews<sup>1</sup>, S. Jachmich<sup>4</sup>, L. Li<sup>1</sup>, P. Lomas<sup>3</sup>, and the JET Contributors<sup>†</sup>

*EUROfusion Consortium, JET, Culham Science Centre, Abingdon, OX14 3DB, UK*

<sup>1</sup>*Forschungszentrum Jülich GmbH, Institut für Energie- und Klimaforschung - Plasmaphysik, 52425 Jülich, Germany*

<sup>2</sup>*Huazhong University of Science and Technology, 430074 Wuhan, China*

<sup>3</sup>*CCFE, Culham Science Centre, Abingdon, OX14 3DB, UK*

<sup>4</sup>*Koninklijke Militaire School-Ecole Royale Militaire, B-1000 Brussels, Belgium*

### Introduction

Active control of Type-I edge-localized mode (ELM) using 3D fields has been demonstrated in several tokamaks [1-5], and it provides an attractive method for ELM control in ITER. To date, more and more experimental results show the plasma response to the 3D perturbation fields is important for understanding the mechanism of ELM control. On JET, it has been found that the plasma response to  $n = 2$  fields measured by saddle loops was saturated during the ramp-up of the current flowing in the error field correction coils (EFCCs) [6]. Recently, the experiment in DIII-D shows rapid increase in the inner-wall magnetic response to an  $n = 2$  field when the plasma transitions into ELM suppression [7].

To further investigate the plasma response to  $n = 2$  fields on JET, the eddy currents in the vacuum vessel induced by the varying of EFCC currents should be taken into account. Since the former work [6] hasn't considered the eddy effect, this paper will focus on the analysis of eddy effect on measured  $n = 2$  field based on a vacuum pulse.

### Experimental setup and eddy current model

JET is equipped with four error field correction coils (EFCCs) outside the vacuum vessel. A set of saddle loops, with 14 toroidal rows and 8 loops in each row, are fitted against the ex-vessel wall. A sketch of EFCCs and saddle loops is shown in Figure 1. Only one low field side row of saddle loops, which will be used for the analysis of eddy effect in this paper, are shown. They are named from S101 to S801, based on their toroidal locations. Using the radial magnetic fields measured by these 8 saddle loops, two orthogonal components of  $n = 2$  field can be calculated, i.e.  $b_r^{\cos} = (b_{S101} - b_{S301} + b_{S501} - b_{S701})/4$  and  $b_r^{\sin} = (b_{S201} - b_{S401} + b_{S601} - b_{S801})/4$ . Then the amplitude of  $n = 2$  field is calculated via  $b_r^{n=2} = \sqrt{(b_r^{\sin})^2 + (b_r^{\cos})^2}$ , and the phase is  $\phi^{n=2} = \text{atan}(b_r^{\sin}/b_r^{\cos})$ .

\* E-mail: wangnc@hust.edu.cn

<sup>†</sup> See the Appendix of F. Romanelli et al., *Proceedings of the 25th IAEA Fusion Energy Conference 2014*, Saint Petersburg, Russia

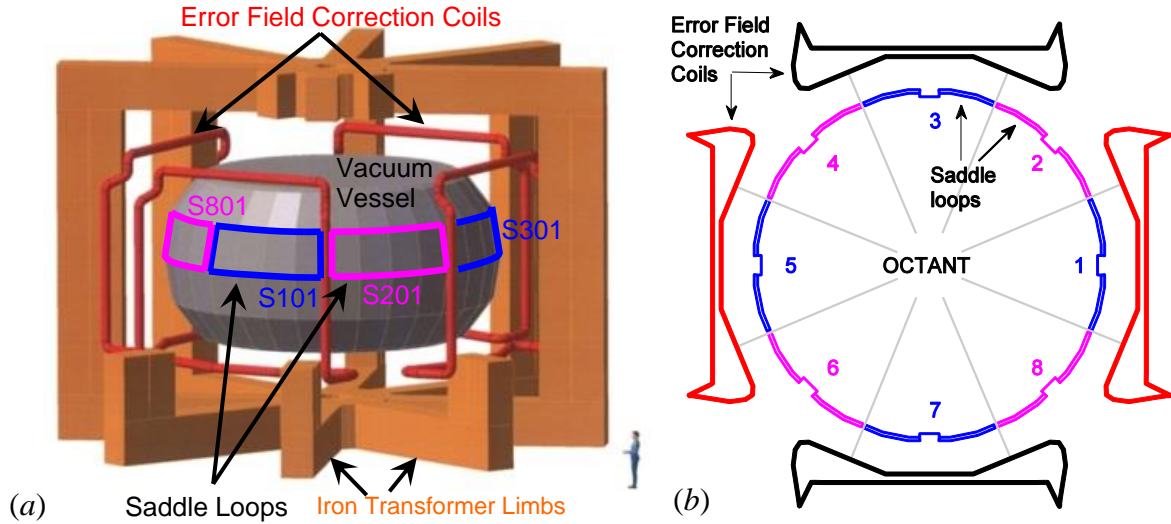


Figure 1 Sketch of the EFCCs and the low field side saddle loops in (a) 3D view and (b) plan view.

In order to obtain the plasma response to applied  $n = 2$  EFCC field, the vacuum field must be removed from the signals of plasma pulses. Since the saddle loops in the odd octants are exactly under the EFCCs as shown in Figure 1(b), the  $b_r^{\cos}$  signal can measure the vacuum fields induced by  $n = 2$  EFCCs, which are significantly larger than the  $n = 2$  field from plasma response. Except for the direct coupling between saddle loops and EFCCs, the eddy currents excited in the vessel by  $dI_{\text{EFCC}}/dt$  can also contribute to the measured  $n = 2$  field. An analytical model has been used to describe the eddy effect on saddle loop measurement on JET. This model was developed to analysis the eddy effect on a single saddle loop on the J-TEXT tokamak [8]. As shown in Figure 3 of Ref. 8, the eddy currents flowing in the vacuum vessel are equivalent to several  $L$ - $R$  circuits which couple with the EFCCs and saddle loops. Neglecting the mutual inductance between eddy circuits and assuming zero state of the system, the analytical solution of this model can be written as

$$b_r = M_{sl} I_s(t) - \sum_{j=1}^k H_e^j \left[ I_s(t) - \left( \exp(-t/\tau_e^j) / \tau_e^j \right) \int_0^t I_s(t) \exp(t/\tau_e^j) dt \right], \quad (1)$$

where  $M$  is the mutual inductance,  $H$  is a parameter relevant with inductances as defined in Ref. 8,  $I$  is the source current, and  $\tau$  is the time constant of eddy circuit. The subscripts  $s$ ,  $l$ ,  $e$  denote the EFCCs, saddle loop, and eddy circuits, and  $k$  is the number of eddy circuits used. The vacuum pick-up induced by the EFCCs and the eddy currents can be identified by fitting Eq. (1) to the signals measured by the saddle loops in a vacuum reference pulse (no plasma).

## Results

JET pulse 82563 is shown in Figure 2 as an example for the application of Eq. (1). After the plasma in pulse 82563 was landed, EFCC current was ramped up at a rate of 1.9 kA/s to the 1.5 kA flattop, and then oscillations with frequencies (amplitudes) of 10 Hz (0.45 kA), 30

Hz (0.15 kA) and 50 Hz (0.05 kA) were superimposed to the flattop. Both the measured  $b_r^{\cos}(n=2)$  and  $b_r^{\sin}(n=2)$  are fitted to the function of  $I_{\text{EFCC}}$  as described by Eq. (1). The parameters  $M$ ,  $H$  and  $\tau$  can be calculated using the nonlinear least square fitting.

The *cosine* component of vacuum  $n = 2$  field from the EFCC coils,  $M \times I_{\text{EFCC}}$ , is shown by the blue line in Figure 2(a), while the vacuum field from all the eddy currents is shown by the magenta line. The sum of these two parts makes up the fitted signal (red line in Figure 2(a)). As a comparison, the original measured signal is shown by the black line. The fitting error between measured and fitted signals is shown in figure 2(c). The eddy current part, shown in magenta line of Figure 2(a), is contributed from 3 eddy circuits with different time constants, i.e. 9.2 ms, 54 ms, and 1.09 s, respectively. The three parts are plotted in Figure 2(b). All the signals are analyzed and plotted in the original acquired frequency of 500 Hz, and haven't been smoothed or filtered. This indicates that the fitting error is so small that it is at the same order as the noise. Hence it is shown that the 3 assumed eddy currents are enough to describe the eddy effect.

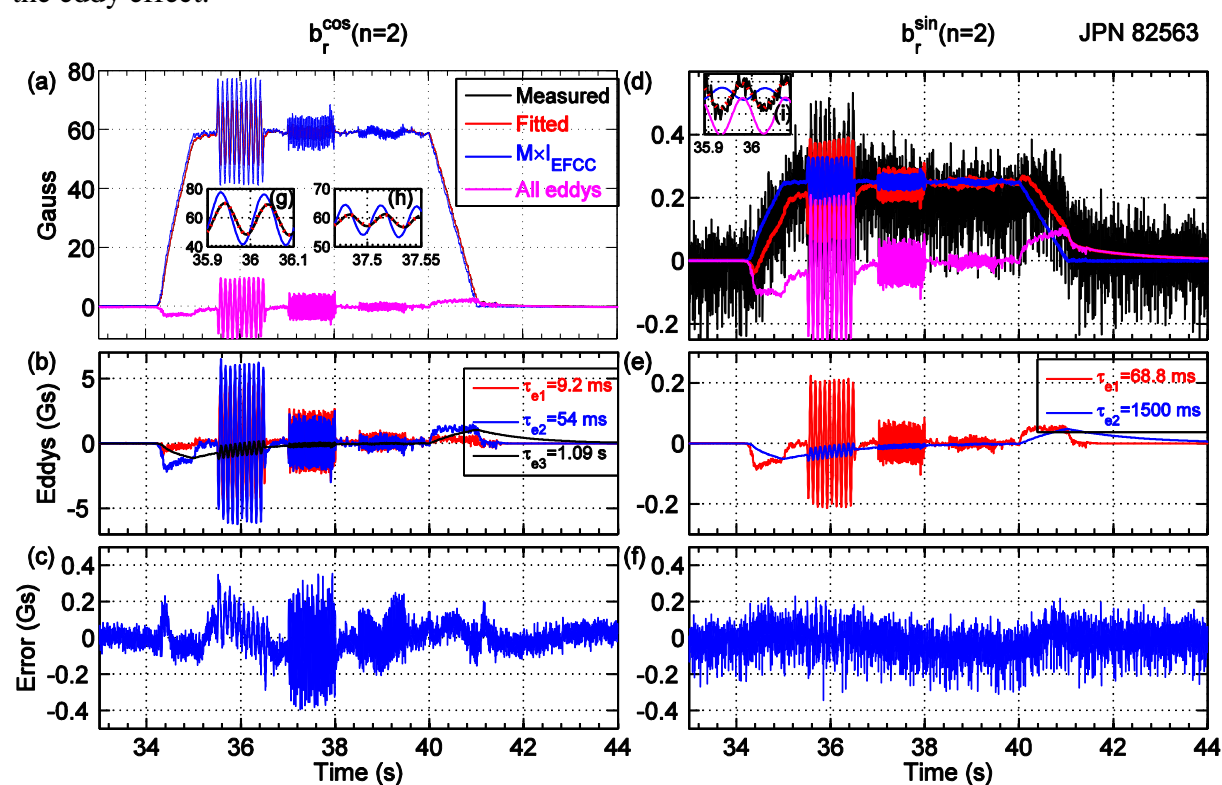


Figure 2 Measured vacuum  $n = 2$  field and the analysis results in a pulse 82563 with  $n = 2$  EFCC.

Figure 2(g) and (h) show the expanded views of measured signals, fitted signals and  $M \times I_{\text{EFCC}}$  with 10 Hz and 30 Hz oscillations. The significant differences between measured signals and  $M \times I_{\text{EFCC}}$  show the large contributions from eddy currents again. The total  $n = 2$  field from all the eddy currents can be as large as 2.5 Gauss during the ramp-up/down of  $I_{\text{EFCC}}$  at around 1.9 kA/s, and around 10 Gauss during the 10 Hz/0.45 kA oscillations.

Figure 2 (d) through (f) show the results for  $b_r^{\sin}(n=2)$  with the same color coding as (a) through (c), and Figure 2 (i) shows the expanded view of Figure 2(d) during the 10 Hz oscillations. Due to the location of even saddle loops and the configuration of EFCC current directions,  $b_r^{\sin}(n=2)$  shows a very small vacuum field during the application of the EFCCs, and two eddy circuits are enough to describe the eddy effect, as shown in Figure 2(e).

Considering the smaller oscillation current at 30 Hz, the fitting error during the 30 Hz oscillation is significantly larger than that of 10 Hz oscillation. Since the higher frequency oscillations can induce eddy current with faster time constant, fast eddy current will be needed in the model. But if the time constant is faster than 10 ms, the integration, expressed by the second part in right hand side of Eq.(1), will result in an unacceptable numerical error for data acquired at 500 Hz. So the time constants are restricted to be larger than 10 ms in the fitting. This may be the reason why the errors for higher frequency oscillations are larger. A higher data acquisition rate is needed to provide better fitting for high frequency oscillations.

## Conclusion and Acknowledgments

An analytical model [8] has been successfully used in analyzing the eddy effect during the application of the EFCC field. The vacuum  $n=2$  field generated by the eddy current with  $dI_{\text{EFCC}}/dt \sim 1.5$  kA/s is around 2.5 Gauss, and  $\sim 10$  Gauss during the 10 Hz/0.45 kA oscillation. The eddy effect can be removed with an error less than  $\pm 0.3$  Gauss. In low-beta H-mode plasmas, the eddy effect due to the conducting vacuum vessel has a similar amplitude as the measured plasma response.

This work has been carried out within the framework of the EUROfusion Consortium and has received funding from the Euratom research and training programme 2014-2018 under grant agreement No 633053. The views and opinions expressed herein do not necessarily reflect those of the European Commission. N.W. is thankful for the support from the China Scholarship Council.

## References

- [1] T. E. Evans *et al.*, *Phys. Rev. Lett.* **92** (2004) 235003.
- [2] Y. Liang *et al.*, *Plasma Phys. Controlled Fusion* **49** (2007) B581.
- [3] A. Kirk *et al.*, *Plasma Phys. Controlled Fusion* **53** (2011) 065011.
- [4] W. Suttrop *et al.*, *Phys. Rev. Lett.* **106** (2011) 225004.
- [5] Y. Jeon *et al.*, *Phys. Rev. Lett.* **109** (2012) 035004.
- [6] Y. Liang *et al.*, *Nucl. Fusion* **53** (2013) 073036.
- [7] R. Nazikian *et al.*, *Phys. Rev. Lett.* **114** (2015) 105002.
- [8] Y. Ding, N. Wang, *et al.*, *Rev. Sci. Instrum.* **85** (2014) 043502.